AGU ADVANCING EARTH AND SPACE SCIENCE

Geophysical Research Letters

RESEARCH LETTER
10.1029/2021GL094032

Special Section:
The Three Major Hurricanes of 2017: Harvey, Irma and Maria

Ground Observation of Negative Sprites Over a Tropical Thunderstorm as the Embryo of Hurricane Harvey (2017)

Yongping Wang[1], Gaopeng Lu[1,2,3], Steven A. Cummer[4], Frankie Lucena[5], Morris B. Cohen[6], Huan Ren[1], Jiagen Li[1], Zhengwei Cheng[7], and Shoubao Zhang[8]

[1]School of Earth and Space Sciences, University of Science and Technology of China, Hefei, China, [2]Key Laboratory of Atmospheric Optics, Anhui Institute of Optics and Fine Mechanics, HFIPS, Chinese Academy of Sciences, Hefei, China, [3]Collaborative Innovation Center on Forecast and Evaluation of Meteorological Disasters, Nanjing University of Information Science and Technology, Nanjing, China, [4]Electrical and Computer Engineering Department, Duke University, Durham, NC, USA, [5]Caribbean TLE Observatory, Cabo Rojo, Puerto Rico, [6]School of Electrical and Computer Engineering, Georgia Institute of Technology, Atlanta, GA, USA, [7]National Space Science Center, State Key Laboratory of Space Weather, Chinese Academy of Sciences, Beijing, China, [8]China Research Institute of Radio Wave Propagation, Qingdao, China

Abstract We report on the observation of six red sprites produced by negative cloud-to-ground (CG) lightning strokes in a tropical thunderstorm that later evolved into Hurricane Harvey (2017). Most of these sprites conformed to the morphological characteristics of typical negative sprites previously observed over continental thunderstorms. The sprite-producing CG strokes were located in or near the deep convection region and their impulse charge moment changes all exceeded −500 C-km. During the sprite generation stage, the CG lightning stroke rate declined and the tropical thunderstorm structure appeared stable. Our analysis suggests that tropical marine meteorological systems, such as tropical disturbances, depressions, and thunderstorms are more likely to be main production systems of negative sprites. The frequent occurrence of 18 gigantic jets produced by the same thunderstorm further indicates that the thundercloud charge structures of sprite-producing oceanic thunderstorms are significantly different from that of continental thunderstorms.

Plain Language Summary The space-borne observations from the ISUAL indicate that there could be a very high proportion (nearly 20%) of negative sprites produced in the ocean. Our previous observations of sprites over Hurricane Matthew (2016) found that all the sprites were produced by positive cloud-to-ground lightning strokes. However, only a few dozen hurricanes occur in the North Atlantic every year. In this paper, we report the observation of six negative sprites over a tropical thunderstorm that is more representative to the typical thunderstorms in the ocean. We speculate that this may be due to that the dynamic structure of the outer rainband of hurricanes is similar to the trailing stratiform of the mesoscale convective systems, while the ordinary oceanic thunderstorms with deep convection cores (as inferred from cold cloud tops and high lightning density) are similar to the continental convective meteorological system. Also, the phenomenon of frequent occurrence of gigantic jets indicates that there was an extensive distribution of middle negative charge in the thundercloud. Therefore, the charge structure is different between oceanic thunderstorms and continental thunderstorms and is likely to play an important role in the production processes of sprites with different polarities.

Key Points:

- All the negative sprites were produced over the deep convection region with cold cloud tops and high lightning density in a tropical storm
- The polarity paradox of sprites may be attributed to the charge structure in the thundercloud and the type of parent lightning
- The frequent occurrence of gigantic jets implies the presence of an extensive negative charge layer in the thundercloud

Correspondence to:
G. Lu,
gaopenglu@gmail.com

Citation:
Wang, Y., Lu, G., Cummer, S. A., Lucena, F., Cohen, M. B., Ren, H., et al. (2021). Ground observation of negative sprites over a tropical thunderstorm as the embryo of Hurricane Harvey (2017). *Geophysical Research Letters*, *48*, e2021GL094032. https://doi.org/10.1029/2021GL094032

Received 27 APR 2021
Accepted 2 JUL 2021

1. Introduction

Sprites are the most prominent members of lightning-induced transient luminous events (TLEs), and they result from the transient electric field (*E*-field) perturbation in the mesosphere driven by energetic cloud-to-ground (CG) lightning strokes with large charge transfer to ground (Pasko et al., 1997). The existing ground-based observations show that in the continental region, sprites are overwhelmingly associated with positive CG strokes, while only a very small fraction (<1%) of sprites are produced by negative CG strokes (e.g., Cummer & Lyons, 2005; Lyons, 1996; Williams et al., 2007).

Negative sprites (namely sprites produced by negative CG strokes) typically appear dimmer than their positive counterpart and terminate at relatively high altitudes (Li et al., 2012). Due to the dependence of streamer development on the duration of charge transfer (Qin et al., 2013), many negative CG strokes

with sprite-producible impulse charge moment change (iCMC, defined as the product of charge transfer to ground within 2 ms after the return stroke and the original height in thunderclouds) might only lead to the occurrence of halos, so a large amount of strong negative CG strokes failed to produce sprites (Lu et al., 2018; Williams et al., 2007).

Although more than 90% of lightning occurs over land (Christian et al., 2003), the satellite observations indicate that sprites that occurred over oceanic thunderstorms show a fairly high proportion of negative sprites (Chen et al., 2008, 2019; Lu et al., 2017), which could be attributed to the fact that oceanic thunderstorms are more efficient in producing CG strokes with high peak currents as well as large charge moment change than their continental counterpart (Chronis et al., 2016; Said et al., 2013). Negative sprites and their parent CG lightning in the ocean are still not well understood in many ways. Therefore, more ground-based observations of sprites over oceanic thunderstorms are desired to understand the difference between oceanic and continental thunderstorms that produce sprites.

Our previous work on Hurricane Matthew (2016) indicated that all sprites were produced by positive CG strokes during slowly weakening to the category-4 hurricane (A. Huang et al., 2018). Based on satellite observations, a large number of sprites occurred over the ocean (Chen et al., 2008, 2019; Lu et al., 2017), while only a few dozen hurricanes occur in the North Atlantic every year. Thus, Matthew with eyewall and rainband convection structures is not a good representation of typical oceanic storms that produces sprites. Here we reported the observation of six negative sprites over the deep convection of a tropical thunderstorm as it passed the north of Venezuela, and analyzed the characteristics of the parent thunderstorm. The results show that tropical marine meteorological systems such as tropical disturbances, depressions, and storms are more likely to be the main producers of negative sprites.

2. Observations and Data

Hurricane Harvey (2017) started as a tropical depression formed at 06 UTC (Coordinated Universal Time) on 17 August 2017 and grew into a tropical thunderstorm 12 h later. The tropical storm moved westward quickly, reaching an initial peak intensity of 40 knots at 00 UTC on 18 August. Increasing wind shear caused the storm to weaken back to a depression at 12 UTC on 19 August, and further degenerated into a tropical wave over the central Caribbean Sea at 18 UTC. Afterward, Harvey moved rapidly to the west-northwest. By 23 August, Harvey regenerated into a tropical depression over the Campeche Bay and rapidly intensified into a category-4 hurricane by 00 UTC on 26 August. Harvey weakened to a tropical storm within 12 h after landfall and then dissipated. The track of Harvey (marked by orange dots) is shown in Figure 1a.

During the TLEs-producing period (04–09 UTC on 19 August), tropical storm Harvey passed about 500 km south of Puerto Rico with 35 knots sustained surface winds and a central pressure of 1,005 hPa, and a total of six sprites were recorded. In addition, the same thunderstorm also produced 18 gigantic jets (GJs) (including trailing jets without developing the branched out top), some of which were also reported by Boggs et al. (2019). The observation instrumentation is comprised of a low-light-level video camera (Watec 902H Ultimate camera, 12-mm F/1.2 lens, 32° horizontal FOV) operated by Frankie Lucena, a scientist, in Puerto Rico (18.05°N, 67.11°W). Sprites also were measured synchronously by an ultralow-frequency (ULF, <1–400 Hz) magnetic field sensor system erected near Duke University (35.97°N, 79.09°W) (Lu et al., 2013) and a very-low-frequency to low-frequency (VLF-LF, 0.5–470 kHz) magnetic field sensor system installed in Baxley (31.88°N, 82.36°W) (M. B. Cohen et al., 2018). All the measurements are synchronized by the GPS with timing accuracy better than 1 μs.

In parallel with these measurements, data from the World-Wide Lightning Location Network (WWLLN) were used to identify the real-time location of CG lightning strokes (Bovalo et al., 2014). The inset on the right side of Figure 1a shows the lightning density distribution of CG strokes. The high-density area of CG strokes can indicate the location of deep convection (Keighton et al., 1991). Magnetic field signals indicate that sprites presented in this study all were induced by negative CG strokes. These causative strokes were at a range of about 230–500 km from Puerto Rico and mainly occurred at the edge of lightning high-density regions, that is, cold cloud tops and convection cores. Figure 1b shows the rate of CG strokes over 5 min interval and the area of cloud top brightness temperature below 210 K in the thunderstorm of our interest.

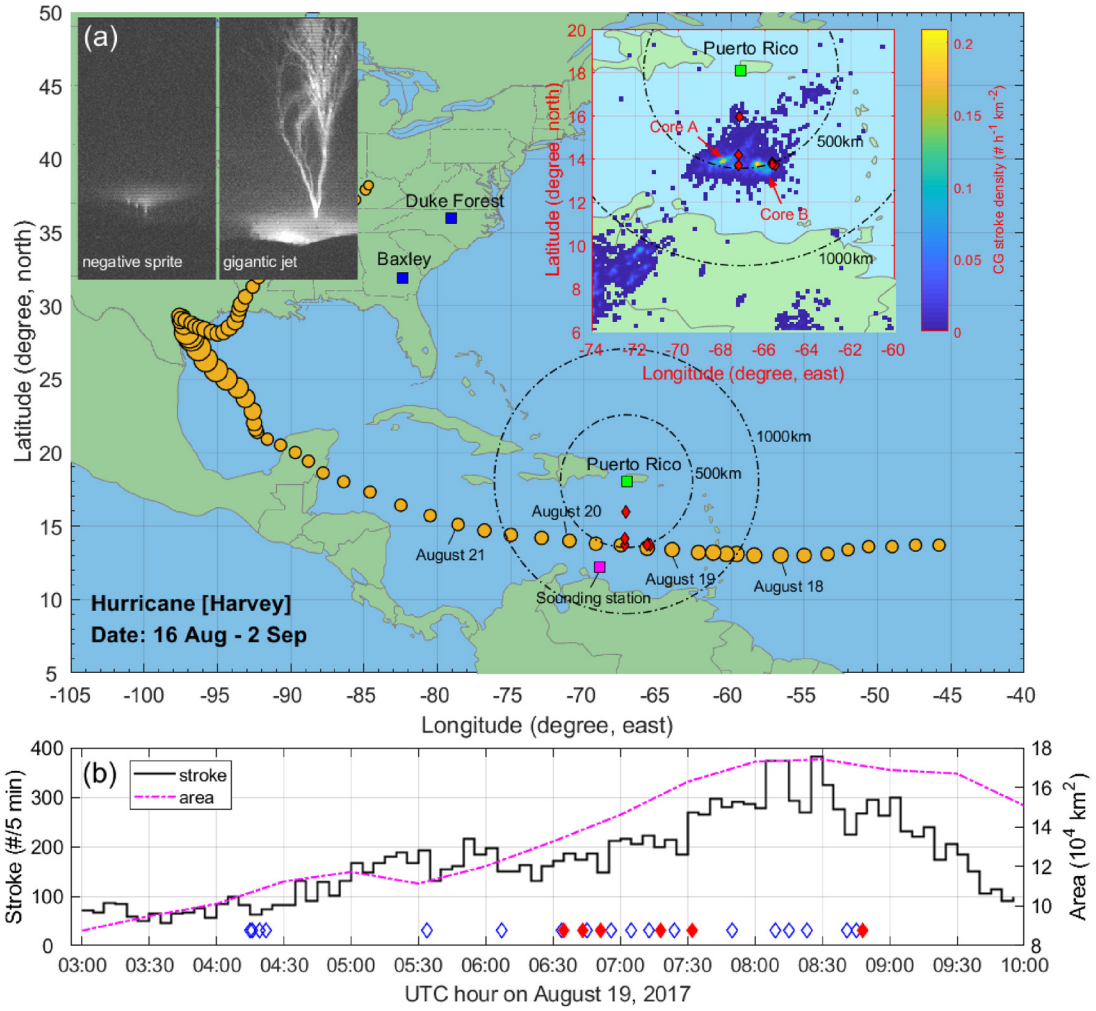

Figure 1. (a) Track of Hurricane Harvey and location of sprite-parent CG strokes detected by World-Wide Lightning Location Network (WWLLN). The orange dots mark the track of Harvey and the radius of dots represents the wind speed of the hurricane; the red diamonds mark the location of parent CG strokes. Black dashed circles mark the circular region with a radius of 500 and 1,000 km centered at Puerto Rico. The left, middle, and right insets represent the sprite image at 0639:46.953 UTC, the gigantic jet image at 0850:16.199 UTC, and the density distribution map of CG strokes, respectively. (b) Rate of CG strokes over 5 min interval and area of cloud top brightness temperature below 210 K. The red diamond symbols show the sprites along with blue open diamond symbols for gigantic jets. CG = cloud-to-ground.

During sprite production, the area with cloud top brightness temperature lower than 210 K is more than 120,000 km^2 and with the increase of 210 K area, the lightning activity is gradually enhanced.

Due to the limited detection range of ground-based radars as well as the low spatial and temporal resolution of satellites, we did not find the available data to directly detect the in-cloud structure. Therefore, this study used the cloud top brightness temperature data (spatial resolution: 2 km at nadir) and the cloud top height data (spatial resolution: 10 km at nadir) from Geostationary Operational Environmental Satellites (GOES), and 91.655-GHz channel (an ice scattering channel) temperature data provided by the Special Sensor Microwave Imager/Sounder aboard Defense Meteorological Satellite Program satellites to analyze the structure and evolution of the tropical thunderstorm. We also investigated sounding data (TNCC station, 12.20°N, 68.96°W) originating from the University of Wyoming and the fifth generation reanalysis data from the European Centre for Medium-Range Weather Forecasts to understand the meteorological environment in more detail.

In addition, we also examined observation data collected by the Geostationary Lightning Mapper (GLM) on board the Geostationary Operational Environmental Satellite-R series. The high orbital altitude of the GLM

enables its charge-coupled device focal plane to continuously observe transient optical pulses with a relatively consistent pixel resolution (spatial resolution increasing from 8 km at nadir to 14 km at the edge of field-of-view) (Goodman et al., 2013; Rudlosky et al., 2018). Different from ordinary lightning that radiates discrete optical pulses, GJs contain continuous optical emissions (tens of ms) and relatively small lateral offset (Boggs et al., 2019). The geographical location of GLM GJs can be determined by matching the GPS time and the azimuth provided by the ground-based observations. It should be noted that sustained strong optical emissions raise the dynamic background radiance, inhibiting continued detection of a pulse and resulting in the shorter duration of GLM GJ detection (Goodman et al., 2013).

3. Analysis and Results

3.1. On the Sprite-Producing Strokes

The images of six negative sprites studied in this paper are shown in Figure 2. The GPS time was encoded onto each video stream by a time inserter with millisecond accuracy. The exposure time of each video field is about 17 ms, so it is not possible to determine the evolution of the events. These sprites almost all obeyed the classic morphology of negative sprites (e.g., Barrington-Leigh et al., 2001; Lu et al., 2016; Taylor et al., 2008). It is noteworthy that event-3 at 0656:29.557 UTC is morphologically more like a positive sprite that appears as clusters of bright column structures extending near-vertically from the mesosphere into the stratosphere and branching at lower elevations. This may be attributed to the large iCMC of the parent lightning stroke. Some dim sprites may not be observed, owing to light crossing through a long-distance atmosphere. By using the method of Hsu et al. (2003), the altitude range of sprites was estimated to be 60–96 km. Since we have assumed that the center of the sprite is located directly above the causative stroke (e.g., Wescott et al., 2001), the offset between sprites and parent lightning strokes is the main cause of the altitude uncertainty.

Figure 2 also shows the associated magnetic field signals. The propagation time of sferic signals over a distance of 2,300–2,800 km have been corrected. Sferic signals indicate that compared to the typical positive counterparts, discharge processes of sprite-producing negative CG strokes had relatively short timescale, and there is no obvious characteristic of millisecond impulse current signature (Li et al., 2012; Lu et al., 2012). Moreover, characteristics of sprite current signal and/or *M*-component signal also were not recorded (Lu et al., 2016). The iCMC is estimated from the ULF data by using the deconvolution method that has been applied extensively in the previous study, which can quantitatively evaluate the capability of a CG stroke to produce sprites (e.g., Cummer & Lyons, 2005). Although the minimum iCMC for triggering negative sprites is estimated to be −320 C·km (Qin et al., 2012), the iCMC of negative sprite-producing CG strokes is usually in excess of −450 C·km (Li et al., 2012). In this paper, estimated iCMCs of parent CG strokes range between −575 and −1572 C·km.

GJs produced by the same thunderstorm exhibited typical morphological features (e.g., S. Huang et al., 2012; Pasko et al., 2002; Su et al., 2003; van der Velde, Bór, et al., 2010). All the reported GJs can be classified as the archetypical tree-like GJ with clearly separated branches and the carrot-like GJ with massive central structure, beads, and patches (van der Velde et al., 2019). Although the low-light-level camera recorded pictures at a relatively low speed, it still clearly reveals the leading jet, fully developed jet, and trailing jet stages of partial events. In addition, Boggs et al. (2019) also examined some of these GJs in detail.

By examining images of TLEs in this paper, it was found that the azimuth of negative sprites relative to the observation site seems to be consistent with that of GJs occurring at a short period. Such association has been noted by previous studies (e.g., Lee et al., 2012, 2013; Marshall & Inan, 2007). van der Velde, Bór, et al. (2010) reported a positive GJ with large charge moment change (11,600 C km) followed about 80 ms by a positive sprite, while some studies indicated that sprites also appeared to influence the occurrence of subsequent jet-like discharges (e.g., Lee et al., 2012; Marshall & Inan, 2007). In particular, Lee et al. (2013) reported that a positive sprite followed within about 30–50 ms by a subsequent GJ, and then about 1 ms after the GJ, a negative sprite occurred near the GJ. They suggest that this may be due to the fact that GJs and sprites mutually provide the favorable electromagnetic environment needed for their generation. The time intervals between sprites and GJs reported in the literature were mostly within 100 ms, while the time intervals in this paper are all about a few minutes. Although the relationship between TLEs is still an open

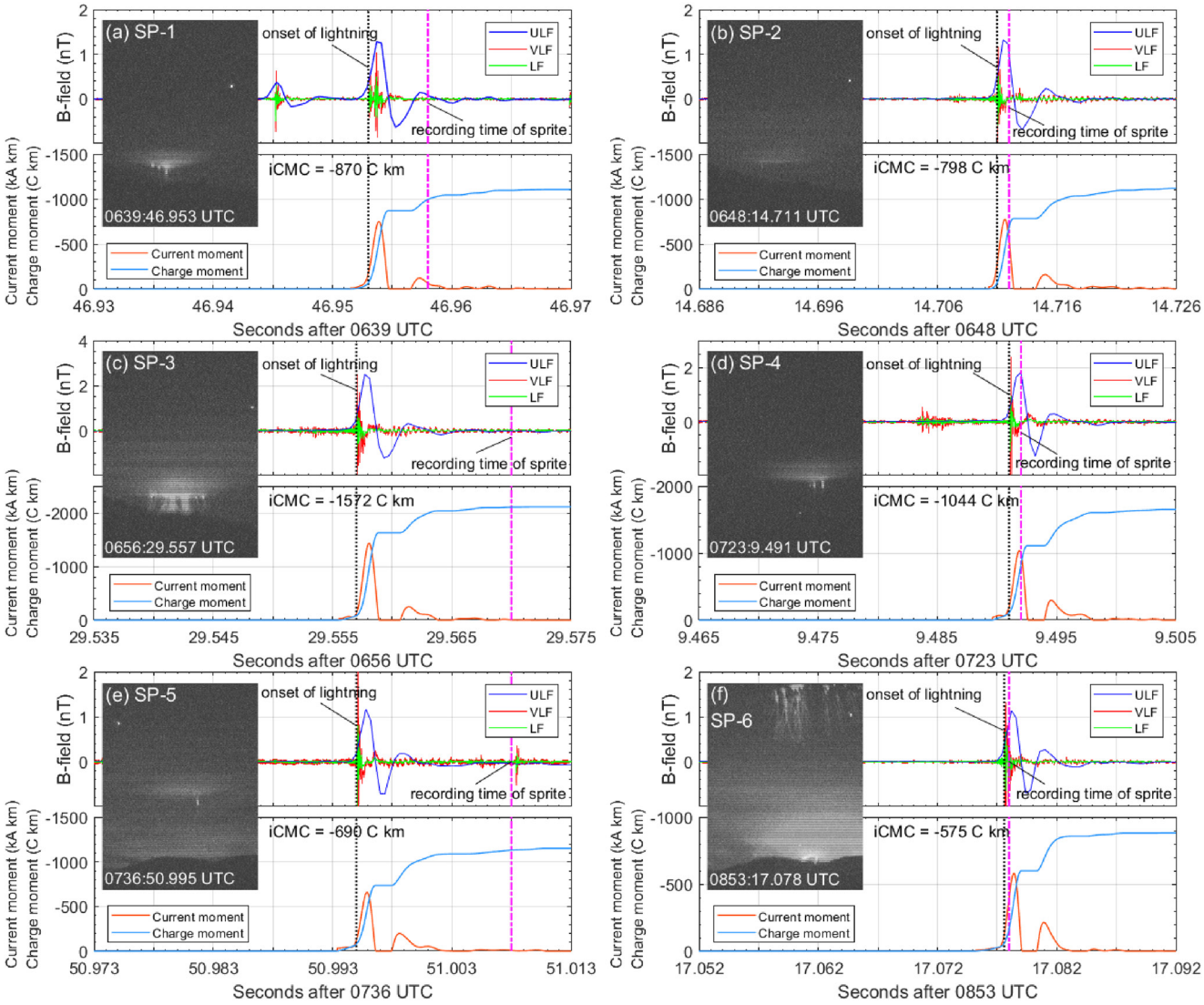

Figure 2. Sprite images captured in Puerto Rico, associated ultralow frequency (ULF, <0.1–400 Hz) magnetic signals recorded in Duke Forest, very low frequency to low frequency (VLF/LF, 0.5–470 kHz) magnetic signals recorded in Baxley, and current moment and cumulated charge moment (change) extracted from the ULF magnetic signals. The time axes of magnetic signals are all corrected by the propagation delay. The onset of the lightning and the recording time of the sprite are indicated by a black dotted-dashed line and a magenta dotted-dashed line, respectively. iCMC = impulse charge moment change.

question, this fact that jet-like discharges and negative sprites appear together in this study should be different from the aforementioned situation.

3.2. On the Parent Thunderstorm

The cloud top brightness temperature can characterize the strong local convection and the rapid cloud top expansion, thus we examined the meteorological morphology and convection system evolution of the parent thunderstorm based on the cloud top brightness temperature. During its transit south of Puerto Rico, the tropical thunderstorm underwent a convective burst between 04 and 09 UTC during which the anvil area substantially increased and the thunderstorm produced more than 13,500 flashes as registered by the WWLLN. Based on the time sequence analysis of cloud top brightness temperature images of GOES, it is found that the overall structure of the thunderstorm changed little when it remained moving fast to the

west. Despite the intense convection, Harvey weakened due to the strong shear and later became a tropical wave.

Figures 3a–3d show the distribution of WWLLN lightning (within 30-min interval centered at the time given in each panel) overlaid on the brightness temperature at four different times. The lowest brightness temperature was about 182–184 K. The spatial distribution of CG strokes and the cloud system shows that lightning activity was predominately located in two vigorous convection regions (brightness temperature ≤194 K), while causative strokes (red open diamonds in Figures 3a–3d) occurred at the edge of deep convection cores, which is consistent with the finding of previous studies (e.g., Boggs et al., 2016; Lang et al., 2013). Interestingly, the negative CG rate in convection cores of the tropical storm relatively decreases during the sprite generation phase (Figure 3e), which may be due to the accumulation of excess negative charge in the cloud, while the positive CG rate has not this correlation.

Because the sprite occurrences are random, it is nearly impossible to make in-situ measurements (e.g., rockets, balloons, etc.). Therefore, we examined the atmospheric profile and the intra-cloud (IC) water phase distribution to evaluate the charge structure of the oceanic thunderstorm. Although both the upward motion (mainly depends on large-scale circulation) and radiative cooling (depends on the concentrations of water vapor and aerosol) are responsible for ice formation in a thunderstorm, the thermal structure of thunderstorms in an oceanic context may be a better preference for ice crystal formation. Figure 3f shows that the tropopause layer is about 16 km, which is consistent with the normal height of the tropical region (Biondi et al., 2012).

Takahashi (1978) suggested that both the magnitude and polarity of the charge reservoir in the cloud are highly dependent on the temperature and cloud water content. The positive charge layer is usually located at altitudes below −40°C, while the negative charge layer is located between −20°C and −40°C (Emersic & Saunders, 2010). In a normally electrified thunderstorm, ice crystals at upper altitudes (about 8–16 km) carry positive charge and rimed graupel at middle altitudes (about 6–8 km) carry negative charges (Guo et al., 2016). As shown in Figure 3g, the water vapor profile at 07 UTC in convection core A shows that there is a larger spacing (about 2–3 km) between −20°C (cloud water layer) and −40°C (cloud ice layer), which provides more room for the development of negatively charged cloud region, thus increasing the amount of main negative charge. Whether this feature will lead to a more extensive main negative charge region in the thundercloud merits further investigations.

The vertical wind field at 07 UTC in convection core A (Figure 3h) shows that the convective core region had a strong wind shear, which could weaken the *E*-field intensity between main negative and positive charge layers through turbulent mixing (Boggs et al., 2016, 2018). Due to the divergence of updrafts at high altitudes, the organized development of hurricanes will be limited when oceanic storms have large wind shear. By comparing vertical wind fields of convection cores at different times as the storm passed over Puerto Rico, it can be seen that the storm maintained strong wind shear during the period of spirits and GJs. Also, the wind shear could horizontally offset the main negative charge region from the main positive charge center (Boggs et al., 2016, 2018). Although the initial IC discharges can neutralize the upper positive and mid-level negative charge, a surplus of mid-level negative charge reservoir still allow a large amount of negative charge to be transported to the ground by the negative leader. Lu et al. (2012) also indicated that this hybrid IC-CG activity is more likely to produce greater iCMCs (about −200 C-km or more) than typical CG strokes.

4. Discussions

Previous studies showed that continental positive sprites often occur above the extensive trailing stratiform region of mesoscale convective systems (MCSs) (e.g., Lang et al., 2010; Lyons, 1996; van der Velde, Montanyà, et al., 2010), while negative sprites are more likely to occur in or near deep convection (e.g., Boggs et al., 2016; Lang et al., 2013). In addition, Lu et al. (2016) showed that the negative sprite can also be induced by consecutive impulse charge transfers. It should be noted that the positive and negative sprite-parent CG strokes can both be located in distinct regions of the same thunderstorm (Lu et al., 2016). However, most of the studies are focused on land/coastal thunderstorms. Characteristics of sprite-producing oceanic storms are still an open question and merit a further investigation.

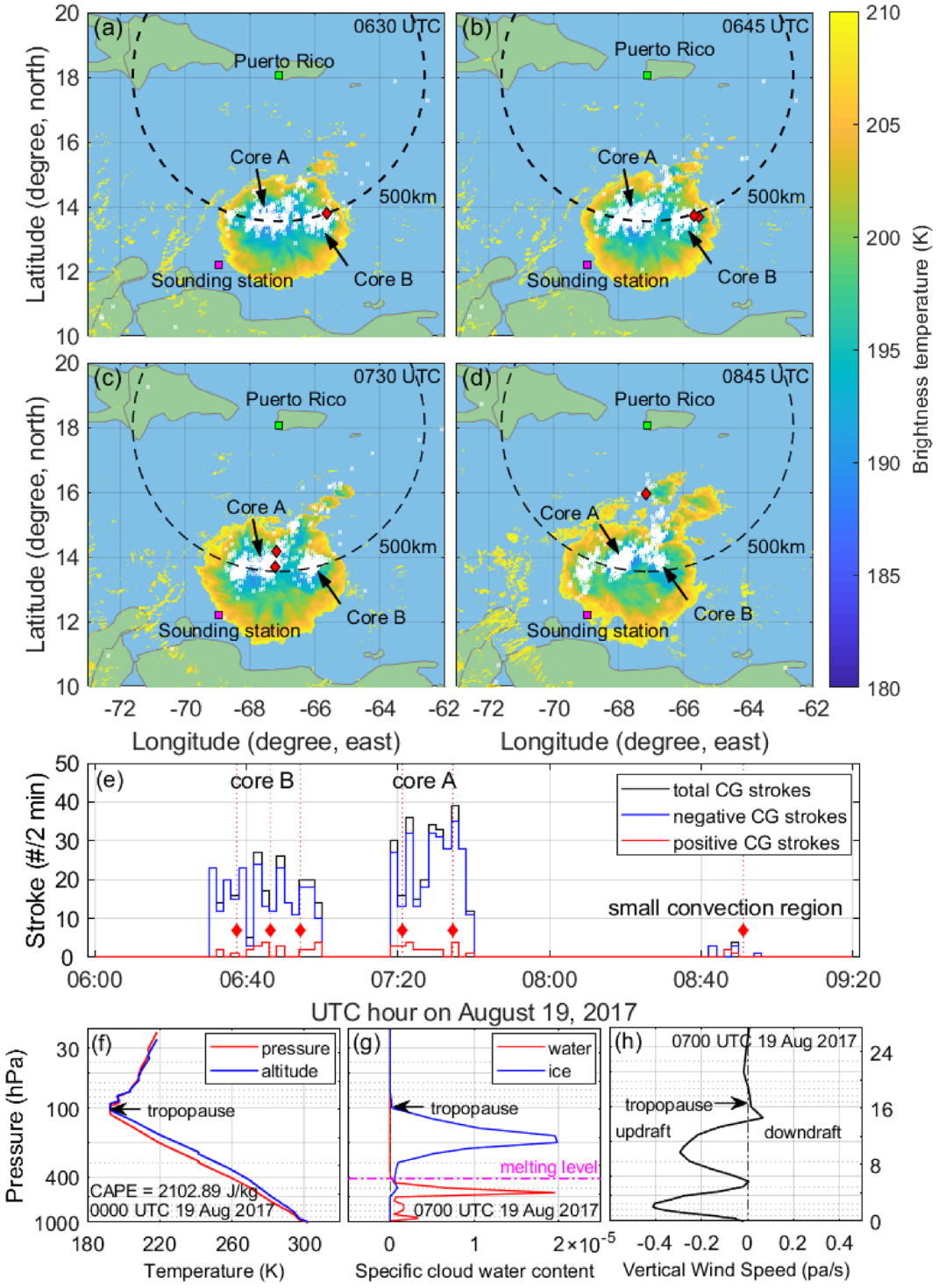

Figure 3. (a–d) Lightning distribution of World-Wide Lightning Location Network (WWLLN) as shown by the combined satellite observations of cloud top brightness temperature during four consecutive time intervals centered at the image time. White crosses mark cloud-to-ground (CG) strokes detected by WWLLN (within 30-min interval centered at the image time), red diamonds mark sprite-parent CG strokes, black dashed circles mark the circular region with a radius of 500 and 1,000 km centered at Puerto Rico, and the pink dashed lines represent the camera field of view. (e) Rate of CG strokes over 2 min interval in convective cores. Red diamond symbols represent sprites. (f) Atmospheric temperature profile at 00 UTC on August 19, 2017. (g) Cloud water content profile at 07 UTC on August 19, 2017. (h) Vertical wind profile at 07 UTC on August 19, 2017.

Thomas et al. (2010) investigated the lightning activity in three hurricanes to evaluate the capability of tropical cyclones to produce sprites. Their analysis revealed that although electromagnetic fields emitted by most of lightning in the eyewall region surpassed the threshold for driving electron density perturbations in the lower ionosphere (80–100 km), they did not spawn sprites. A. Huang et al. (2018) reported that sprites captured over Hurricane Matthew (2016) were all produced by positive CG strokes in the outer rainbands, and the outer rainbands hosting the sprites exhibited a quasi-circular structure similar to MCSs. S. Huang et al. (2012) also reported the observation of sprites above Typhoon Lionrock (2010), but unfortunately, they did not verify polarities of sprite-producing strokes. However, tropical cyclones are not frequent oceanic meteorological systems. A significant proportion of negative sprites were observed by space-borne platforms in oceanic thunderstorms (e.g., Chen et al., 2019; Lu et al., 2017). Williams et al. (2012) also indicated that only negative sprites have been observed in the vast oceanic area to the north of Venezuela. Interestingly, the thunderstorm of our interest also occurred at this region, and only produced negative sprites. We speculate that this may be due to that the dynamic structure of the outer rainband of hurricanes is similar to the trailing stratiform of the MCSs, while the ordinary oceanic thunderstorms with deep convection cores (as inferred from cold cloud tops and high lightning density) are similar to the continental convective meteorological system. The charge structure of thunderstorms may play an important role in the production of sprites with different polarities.

The sprites and GJs detected from 0400 to 0830 UTC occurred in association with the deep convection (cold cloud tops and large lightning densities) near the thunderstorm center, while the last three cases (before 0900 UTC) occurred within a small convection region 250 km north of the thunderstorm center. This may better indicate that the charge structure in the cloud is the main reason for the occurrence of sprites/GJs, rather than the thunderstorm type. In addition, the frequent presence of GJs indicates that there is a large middle negative charge in the thundercloud (Boggs et al., 2018). Figures 4a and 4b show the sprite-parent stroke location (0853:17.078 UTC) and the GLM GJ location (0850:16.283 UTC) overlaid on the 91.665-GHz channel temperature image and the cloud top height image of GOES, respectively. By comparing Figures 4a and 4b, we can see that the sprite-parent stroke and the GLM GJ both appear near the cold cloud top (around 195 K) of the small convective region on the north side (Figure 4a). The low temperature region of the 91.665-GHz channel is not completely consistent with the high value region of cloud top height, and the lowest temperature region is located to the west side of the highest cloud top region. This indicate that the ice layer center and the liquid water layer center is likely to be asymmetrical. The GJ is closer to the ice layer center than the sprite. When oceanic storms have large wind shear, it is conducive to the generation of sprites and GJs. The inset of Figure 4b shows that the vertical wind field where the sprite occurred has a large wind shear, which promotes explosive updrafts/downdrafts. The meridional wind is easterly, which is consistent with the offset direction of the ice layer. In addition, the lightning activity (0845–0900 UTC) during the TLEs was not vigorous in the small convection region. This may also be related to the change of charge structure in the thundercloud.

However, there seems to be no correlation between the occurrence time of sprites and GJs. Boggs et al. (2016) indicated that after IC discharges, the initial state of upper and lower positive charge in the thundercloud determines the initiation and propagation of the subsequent negative leader. Negative leaders generally move in the direction of the largest positive potential gradient. The following negative leader will develop into negative CG lightning when the lower positive charge is larger, and it will force the main negative charge layer to couple with the mesosphere and form the jet-like discharges while when the upper positive charge is larger (Krehbiel et al., 2008). Therefore, there are good reasons to believe that the companion occurrence of jet-like discharges and negative sprites is mainly due to the same charge structure in the cloud, not only because they mutually provide the favorable electromagnetic environment needed for their generation.

Although this study cannot provide discharge patterns in the thundercloud, it is plausible to speculate that the charge structure of the tropical thunderstorm examined in this paper is similar to that reported by Boggs et al. (2016). The verification of the idea requires multi-instrument observations in the future including lightning channel mapping. Furthermore, this situation is not unique in tropical depression/disturbance systems. Liu, Spiva, et al. (2015) and Lazarus et al. (2015) documented the observation of seven upward jet-like discharges (including two blue jets and four GJs) above the convection region of tropical depression

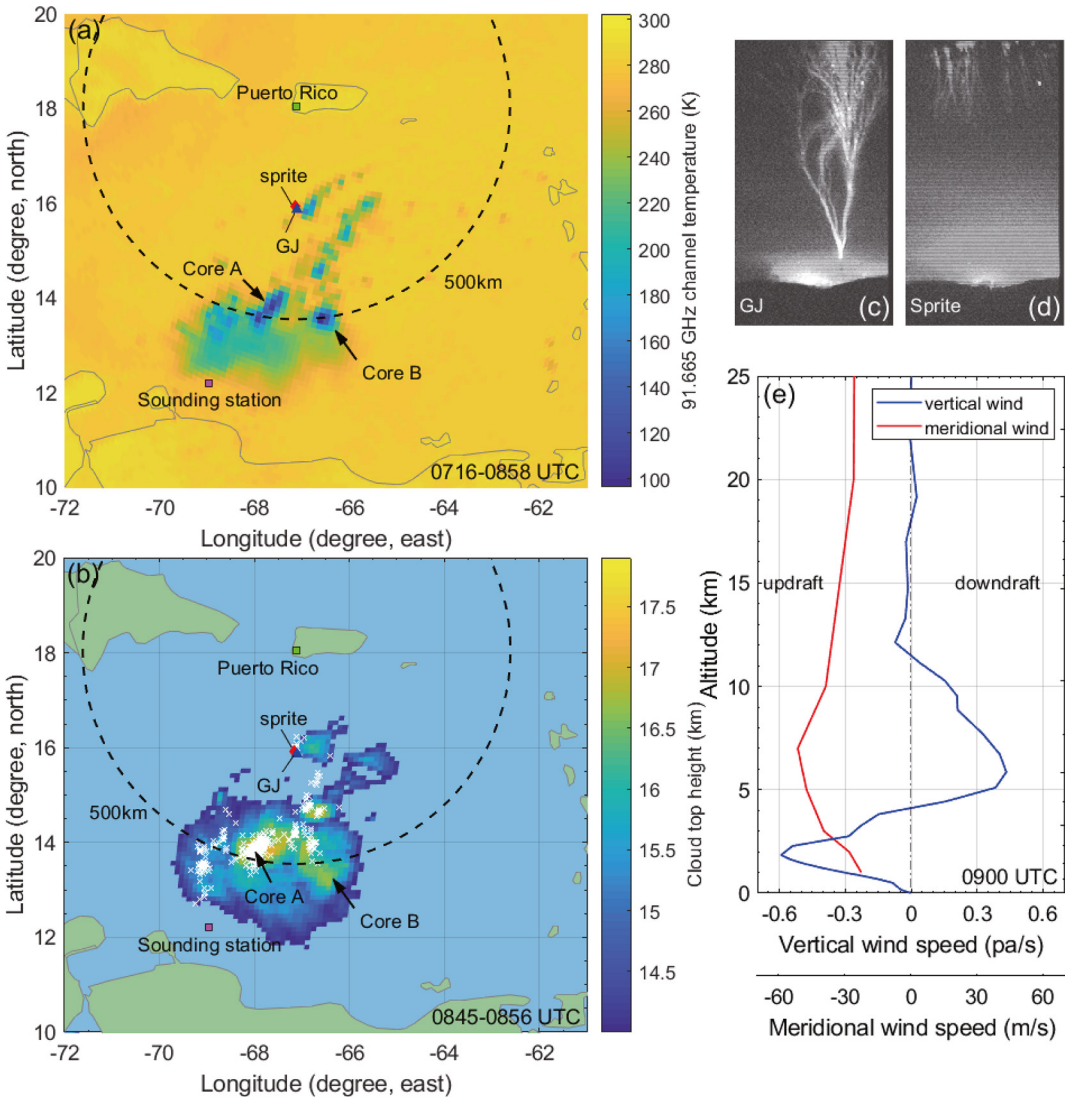

Figure 4. (a) The image of 91.665-GHz channel temperature at 0716–0858 UTC on August 19, 2017. The red diamond and the blue triangle represents the sprite-parent cloud-to-ground (CG) stroke and the gigantic jet. The black dashed circle marks the circular region with a radius of 500 km centered at Puerto Rico. (b) The image of cloud top height at 0845–0856 UTC on August 19, 2017. The red diamond and the blue triangle represents the sprite-parent CG stroke and the gigantic jet. White crosses mark CG strokes detected by WWLLN near the parent CG stroke from 0845 to 0900 UTC. The black dashed circle marks the circular region with a radius of 500 km centered at Puerto Rico. (c–d) The sprite image at 0853:17.078 UTC and the gigantic jet image at 0850:16.199 UTC, respectively. (e) Profiles of cloud ice water content and cloud liquid water content at 0900 UTC near the occurrence region of the sprite and gigantic jet.

Dorian on August 3, 2013. Although they did not report sprites, it is still worthy of reference. In addition, the oceans seem to be more prone to produce the electromagnetic environment for inducing sprites/GJs. For instance, atmospheric gravity waves caused by hurricanes may lead to in-homogeneities in the mesosphere, which is conducive to the initiation of sprites or jet-like discharges (Liu, Dwyer, et al., 2015, 2016). Therefore, it will improve the comprehensive understanding on the meteorological and electrical properties of the sprite-parent storms to study the role of oceanic thunderstorms in the global circuit.

5. Conclusions

In this paper, we analyzed six sprites that were all produced by negative CG strokes over a tropical thunderstorm, with a purpose to reveal the typical meteorological system that produces negative sprites in the ocean.

Based on the cloud top brightness temperature and lightning location data, the sprite-parent CG strokes occurred at the edge of deep convection cores (as inferred from cold cloud tops and high lightning density). We suggest that charge structure differences of sprite-parent thunderstorms may be responsible for differences in sprite polarity over the ocean and land, and tropical marine meteorological systems such as tropical disturbances, depressions, and storms are more likely to be the main producers of negative sprites. In addition, we recorded 18 GJs, while nearly all reported GJs occurred in maritime tropical environments (e.g., Boggs et al., 2019; S. Huang et al., 2012; Lazarus et al., 2015). This further indicates that the charge structure of sprite-producing oceanic thunderstorms may be significantly different from that of continental thunderstorms.

The present work further complements observations of negative sprites over oceanic thunderstorms. Due to the absence of available data, the issue of charge structures and discharge patterns of sprite-producing oceanic thunderstorms still remains to be verified. Further observation experiments and numerical simulations should be carried out to resolve this issue in future work.

Data Availability Statement

The Watec 902HU camera system, which was used to record the events in this paper, was purchased by John Mathews of Penn State University under NSF grant 12-02019. VLF/LF data are available on the WALDO repository at http://waldo.world (M. Cohen, 2020). The data used for the analyses in this paper are available at https://zenodo.org/record/4709704#.YIFsyKG-taQ.

Acknowledgments
This work was supported by the National Key Research and Development Program of China (2019YFC1510103), the CAS Project of Stable Support for Youth Team in Basic Research Field (YSBR-018), the National Natural Science Foundation of China (41622501 and U1938115), the Chinese Meridian Project, and the International Partnership Program of Chinese Academy of Sciences (183311KYSB20200003). We gratefully acknowledge the environmental data (brightness temperature, cloud top height, and geostationary lightning mapper) from Geostationary Operational Environmental Satellites, lightning data provided by the World-Wide Lightning Location Network, 91.655-GHz channel temperature data provided by the Special Sensor Microwave Imager/Sounder aboard Defense Meteorological Satellite Program satellites, and meteorological data originating from the University of Wyoming and the European Centre for Medium-Range Weather Forecasts. We express great gratitude to two reviewers for their careful work and thoughtful suggestions that have helped improve this paper substantially.

References

Barrington-Leigh, C. P., Inan, U. S., & Stanley, M. (2001). Identification of sprites and elves with intensified video and broadband array photometry. *Journal of Geophysical Research*, *106*(A2), 1741–1750. https://doi.org/10.1029/2000JA000073

Biondi, R., Randel, W. J., Ho, S.-P., Neubert, T., & Syndergaard, S. (2012). Thermal structure of intense convective clouds derived from GPS radio occultations. *Atmospheric Chemistry and Physics*, *12*, 5309–5318. https://doi.org/10.5194/acp-12-5309-2012

Boggs, L. D., Liu, N., Peterson, M., Lazarus, S., Splitt, M., Lucena, F., et al. (2019). First observations of gigantic jets from geostationary orbit. *Geophysical Research Letters*, *46*, 3999–4006. https://doi.org/10.1029/2019GL082278

Boggs, L. D., Liu, N., Riousset, J. A., Shi, F., Lazarus, S., Splitt, M., & Rassoul, H. K. (2018). Thunderstorm charge structures producing gigantic jets. *Scientific Reports*, *8*, 18085. https://doi.org/10.1038/s41598-018-36309-z

Boggs, L. D., Liu, N., Splitt, M., Lazarus, S., Glenn, C., Rassoul, H., & Cummer, S. A. (2016). An analysis of five negative sprite-parent discharges and their associated thunderstorm charge structures. *Journal of Geophysical Research - D: Atmospheres*, *121*, 759–784. https://doi.org/10.1002/2015JD024188

Bovalo, C., Barthe, C., Yu, N., Yu, N., & Begue, N. (2014). Lightning activity within tropical cyclones in the South West Indian Ocean. *Journal of Geophysical Research - D: Atmospheres*, *119*, 8231–8244. https://doi.org/10.1002/2014JD021651

Chen, A. B.-C., Chen, H., Chuang, C.-W., Cummer, S. A., Lu, G., Fang, H.-K., et al. (2019). On negative sprites and the polarity paradox. *Geophysical Research Letters*, *46*, 9370–9378. https://doi.org/10.1029/2019GL083804

Chen, A. B.-C., Kuo, C.-L., Lee, Y.-J., Su, H.-T., Hsu, R.-R., Chern, J.-L., et al. (2008). Global distributions and occurrence rates of transient luminous events. *Journal of Geophysical Research*, *113*, A08306. https://doi.org/10.1029/2008JA013101

Christian, H. J., Blakeslee, R. J., Boccippio, D. J., Boeck, W. L., Buechler, D. E., Driscoll, K. T., et al. (2003). Global frequency and distribution of lightning as observed from space by the Optical Transient Detector. *Journal of Geophysical Research*, *108*(D1), 4005. https://doi.org/10.1029/2002JD002347

Chronis, T., Koshak, W., & McCaul, E. (2016). Why do oceanic negative cloud-to-ground lightning exhibit larger peak current values? *Journal of Geophysical Research - D: Atmospheres*, *121*, 4049–4068. https://doi.org/10.1002/2015JD024129

Cohen, M. (2020). Returning lightning data to the cloud. *Eos*, *101*. https://doi.org/10.1029/2020EO142801

Cohen, M. B., Said, R. K., Paschal, E. W., McCormick, J. C., Gross, N. C., Thompson, L., et al. (2018). Broadband longwave radio remote sensing instrumentation. *Review of Scientific Instruments*, *89*(9), 094501. https://doi.org/10.1063/1.5041419

Cummer, S. A., & Lyons, W. A. (2005). Implications of lightning charge moment changes for sprite initiation. *Journal of Geophysical Research*, *110*, A04304. https://doi.org/10.1029/2004JA010812

Emersic, C., & Saunders, C. (2010). Further laboratory investigations into the relative diffusional growth rate theory of thunderstorm electrification. *Atmospheric Research*, *98*(2-4), 327–340. https://doi.org/10.1016/j.atmosres.2010.07.011

Goodman, S. J., Blakeslee, R. J., Koshak, W. J., Mach, D., Bailey, J., Buechler, D., et al. (2013). The GOES-R geostationary lightning mapper (GLM). *Atmospheric Research*, *125*, 34–49. https://doi.org/10.1016/j.atmosres.2013.01.006

Guo, F., Lu, G., Wu, X., Wang, H., Liu, Z., Bao, M., & Li, Y. (2016). Occurrence conditions of positive cloud-to-ground flashes in severe thunderstorms. *Science China Earth Sciences*, *59*(7), 1401–1413. https://doi.org/10.1007/s11430-016-5279-7

Hsu, R. R., Su, H. T., Chen, A. B., Lee, L. C., Asfur, M., Price, C., & Yair, Y. (2003). Transient luminous events in the vicinity of Taiwan. *Journal of Atmospheric and Solar-Terrestrial Physics*, *65*(5), 561–566. https://doi.org/10.1016/s1364-6826(02)00320-6

Huang, A., Lu, G., Yue, J., Lyons, W. A., Lucena, F., Lyu, F., et al. (2018). Observations of sprites produced above Hurricane Matthew. *Geophysical Research Letters*, *45*. https://doi.org/10.1029/2018GL079576

Huang, S., Hsu, R., Lee, L., Su, H., Kuo, C., Wu, C., et al. (2012). Optical and radio signatures of negative gigantic jets: Cases from Typhoon Lionrock (2010). *Journal of Geophysical Research*, *117*(8). https://doi.org/10.1029/2012ja017600

Keighton, S. J., Bluestein, H. B., & MacGorman, D. R. (1991). The evolution of a severe mesoscale convective system: Cloud-to-ground/lightning location and storm structure. *Monthly Weather Review*, *119*(7), 1533–1556. https://doi.org/10.1175/1520-0493(1991)119<1533:TEOASM>2.0.CO;2

Krehbiel, P. R., Riousset, J. A., Pasko, V. P., Thomas, R. J., Rison, W., Stanley, M. A., & Edens, H. E. (2008). Upward electrical discharges from thunderstorms. *Nature Geoscience*, *1*, 233–237. https://doi.org/10.1038/ngeo162

Lang, T. J., Cummer, S. A., Rutledge, S. A., & Lyons, W. A. (2013). The meteorology of negative cloud-to-ground lightning strokes with large charge moment changes: Implications for negative sprites. *Journal of Geophysical Research - D: Atmospheres*, *118*, 7886–7896. https://doi.org/10.1002/jgrd.50595

Lang, T. J., Lyons, W. A., Rutledge, S. A., Meyer, J. D., MacGorman, D. R., & Cummer, S. A. (2010). Transient luminous events above two mesoscale convective systems: Storm structure and evolution. *Journal of Geophysical Research*, *115*(A5), A00E22. https://doi.org/10.1029/2009JA014500

Lazarus, S., Splitt, M., Brownlee, J., Spiva, N., & Liu, N. (2015). A thermodynamic, kinematic and microphysical analysis of a jet and gigantic jet-producing Florida thunderstorm. *Journal of Geophysical Research - D: Atmospheres*, *120*, 8469–8490. https://doi.org/10.1002/2015JD023383

Lee, L.-J., Hsu, R.-R., Su, H.-T., Huang, S.-M., Chou, J.-K., Kuo, C.-L., et al. (2013). Secondary gigantic jets as possible inducers of sprites. *Geophysical Research Letters*, *40*, 1462–1467. https://doi.org/10.1002/grl.50300

Lee, L.-J., Huang, S.-M., Chou, J.-K., Kuo, C.-L., Chen, A. B., Su, H.-T., et al. (2012). Characteristics and generation of secondary jets and secondary gigantic jets. *Journal of Geophysical Research*, *117*, A06317. https://doi.org/10.1029/2011JA017443

Li, J., Cummer, S., Lu, G., & Zigoneanu, L. (2012). Charge moment change and lightning-driven electric fields associated with negative sprites and halos. *Journal of Geophysical Research*, *117*, A09310. https://doi.org/10.1029/2012JA017731

Liu, N., Dwyer, J. R., Stenbaek-Nielsen, H. C., & McHarg, M. G. (2015). Sprite streamer initiation from natural mesospheric structures. *Nature Communications*, *6*(1), 1–9. https://doi.org/10.1038/ncomms8540

Liu, N., Spiva, N., Dwyer, J. R., Rassoul, H. K., Free, D., & Cummer, S. A. (2015). Upward electrical discharges observed above Tropical Depression Dorian. *Nature Communications*, *6*(1), 5995. https://doi.org/10.1038/ncomms6995

Liu, N. Y., Boggs, L. D., & Cummer, S. A. (2016). Observation-constrained modeling of the ionospheric impact of negative sprites. *Geophysical Research Letters*, *43*, 2365–2373. https://doi.org/10.1002/2016GL068256

Lu, G., Cummer, S. A., Blakeslee, R. J., Weiss, S., & Beasley, W. H. (2012). Lightning morphology and impulse charge moment change of high peak current negative strokes. *Journal of Geophysical Research*, *117*(D4), D04212. https://doi.org/10.1029/2011JD016890

Lu, G., Cummer, S. A., Chen, A. B., Lyu, F., Li, D., Liu, F., et al. (2017). Analysis of lightning strokes associated with sprites observed by ISUAL in the vicinity of North America. *TAO: Terrestrial, Atmospheric and Oceanic Sciences*, *28*(4), 5. https://doi.org/10.3319/tao.2017.03.31.01

Lu, G., Cummer, S. A., Li, J., Zigoneanu, L., Lyons, W. A., Stanley, M. A., et al. (2013). Coordinated observations of sprites and in-cloud lightning flash structure. *Journal of Geophysical Research - D: Atmospheres*, *118*, 6607–6632. https://doi.org/10.1002/jgrd.50459

Lu, G., Cummer, S. A., Tian, Y., Zhang, H., Lyu, F., Wang, T., et al. (2016). Sprite produced by consecutive impulse charge transfers following a negative stroke: Observation and simulation. *Journal of Geophysical Research - D: Atmospheres*, *121*(8), 4082–4092. https://doi.org/10.1002/2015JD024644

Lu, G., Yu, B., Cummer, S. A., Peng, K.-M., Chen, A. B., Lyu, F., et al. (2018). On the causative strokes of halos observed by ISUAL in the vicinity of North America. *Geophysical Research Letters*, *45*, 10781–10789. https://doi.org/10.1029/2018GL079594

Lyons, W. A. (1996). Sprite observations above the U.S. High Plains in relation to their parent thunderstorm systems. *Journal of Geophysical Research*, *101*(D23), 29641–29652. https://doi.org/10.1029/96JD01866

Marshall, R. A., & Inan, U. S. (2007). Possible direct cloud-to-ionosphere current evidenced by sprite-initiated secondary TLEs. *Geophysical Research Letters*, *34*, L05806. https://doi.org/10.1029/2006GL028511

Pasko, V. P., Inan, U. S., Bell, T. F., & Taranenko, Y. N. (1997). Sprites produced by quasi-electrostatic heating and ionization in the lower ionosphere. *Journal of Geophysical Research*, *102*(A3), 4529–4561. https://doi.org/10.1029/96JA03528

Pasko, V. P., Stanley, M. A., Mathews, J. D., Inan, U. S., & Wood, T. G. (2002). Electrical discharge from a thundercloud top to the lower ionosphere. *Nature*, *416*(6877), 152–154. https://doi.org/10.1038/416152a

Qin, J., Celestin, S., & Pasko, V. P. (2012). Minimum charge moment change in positive and negative cloud to ground lightning discharges producing sprites. *Geophysical Research Letters*, *39*, L22801. https://doi.org/10.1029/2012GL053951

Qin, J., Celestin, S., & Pasko, V. P. (2013). Dependence of positive and negative sprite morphology on lightning characteristics and upper atmospheric ambient conditions. *Journal of Geophysical Research: Space Physics*, *118*, 2623–2638. https://doi.org/10.1029/2012JA017908

Rudlosky, S. D., Goodman, S. J., Virts, K. S., & Bruning, E. C. (2018). Initial geostationary lightning mapper observations. *Geophysical Research Letters*, *46*, 1097–1104. https://doi.org/10.1029/2018GL081052

Said, R. K., Cohen, M. B., & Inan, U. S. (2013). Highly intense lightning over the oceans: Estimated peak currents from global GLD360 observations. *Journal of Geophysical Research: Atmospheres*, *118*, 6905–6915. https://doi.org/10.1002/jgrd.50508

Su, H. T., Hsu, R. R., Chen, A. B., Wang, Y. C., Hsiao, W. S., Lai, W. C., et al. (2003). Gigantic jets between a thundercloud and the ionosphere. *Nature*, *423*, 974–976. https://doi.org/10.1038/nature01759

Takahashi, T. (1978). Riming electrification as a charge generation mechanism in thunderstorms. *Journal of the Atmospheric Sciences*, *35*(8), 1536–1548. https://doi.org/10.1175/1520-0469(1978)035%3C1536:REAACG%3E2.0.CO;2

Taylor, M. J., Bailey, M. A., Pautet, P. D., Cummer, S. A., Jaugey, N., Thomas, J. N., et al. (2008). Rare measurements of a sprite with halo event driven by a negative lightning discharge over Argentina. *Geophysical Research Letters*, *35*, L14812. https://doi.org/10.1029/2008GL033984

Thomas, J. N., Solorzano, N. N., Cummer, S. A., & Holzworth, R. H. (2010). Polarity and energetics of inner core lightning in three intense North Atlantic hurricanes. *Journal of Geophysical Research*, *115*, A00E15. https://doi.org/10.1029/2009JA014777

van der Velde, O. A., Bór, J., Li, J., Cummer, S. A., Arnone, E., Zanotti, F., et al. (2010). Multi-instrumental observations of a positive gigantic jet produced by a winter thunderstorm in Europe. *Journal of Geophysical Research*, *115*, D24301. https://doi.org/10.1029/2010JD014442

van der Velde, O. A., Montanyà, J., López, J. A., & Cummer, S. A. (2019). Gigantic jet discharges evolve stepwise through the middle atmosphere. *Nature Communications*, *10*, 4350. https://doi.org/10.1038/s41467-019-12261-y

van der Velde, O. A., Montanyà, J., Soula, S., Pineda, N., & Bech, J. (2010). Spatial and temporal evolution of horizontally extensive lightning discharges associated with sprite-producing positive cloud-to-ground flashes in northeastern Spain. *Journal of Geophysical Research*, *115*, A00E56. https://doi.org/10.1029/2009JA014773

Wescott, E. M., Stenbaek-Nielsen, H. C., Sentman, D. D., Heavner, M. J., Moudry, D. R., & São Sabbas, F. T. (2001). Triangulation of sprites, associated halos and their possible relation to causative lightning and micrometeors. *Journal of Geophysical Research*, *106*, 10467–10477. https://doi.org/10.1029/2000JA000182

Williams, E., Downes, E., Boldi, R., Lyons, W., & Hechman, S. (2007). Polarity asymmetry of sprite-producing lightning: A paradox? *Radio Science*, *42*, RS2S17. https://doi.org/10.1029/2006RS003488

Williams, E., Kuo, C.-L., Bór, J., Sátori, G., Newsome, R., Adachi, T., et al. (2012). Resolution of the sprite polarity paradox: The role of halos. *Radio Science*, *47*, RS2002. https://doi.org/10.1029/2011RS004794